2-8-2016

# Continuous Measurements of Dissolved Ne, Ar, Kr, and Xe Ratios with a Field-deployable Gas Equilibration Mass Spectrometer

Cara C. Manning

Rachel H.R. Stanley
rstanle2@wellesley.edu

Dempsey E. Lott III



**Version: Post-print**

Recommended Citation
Manning, CC, RHR Stanley, DE Lott (2016) Continuous measurements of dissolved Ne, Ar, Kr, and Xe ratios with a field-deployable gas equilibration mass spectrometer. Anal. Chem., 2016, 88 (6), 3040–3048. DOI: 10.1021/acs.analchem.5b03102

# Continuous Measurements of Dissolved Ne, Ar, Kr, and Xe Ratios with a Field-deployable Gas Equilibration Mass Spectrometer

Cara C. Manning,[*,†,‡] Rachel H. R. Stanley,[¶] and Dempsey E. Lott III[‡]

*Massachusetts Institute of Technology/Woods Hole Oceanographic Institution Joint Program in Oceanography, Woods Hole, MA, Department of Marine Chemistry and Geochemistry, Woods Hole Oceanographic Institution, Woods Hole, MA, and Department of Chemistry, Wellesley College, Wellesley, MA*

E-mail: cmanning@whoi.edu

**Abstract**

Noble gases dissolved in natural waters are useful tracers for quantifying physical processes. Here, we describe a field-deployable gas equilibration mass spectrometer (GEMS) that provides continuous, real-time measurements of Ne, Ar, Kr, and Xe mole ratios in natural waters. Gas is equilibrated with a membrane contactor cartridge and measured with a quadrupole mass spectrometer, after in-line purification with reactive metal alloy getters. We use an electron energy of 35 V for Ne to eliminate isobaric interferences, and a higher electron energy for the other gases to improve sensitivity. The precision is 0.7 % or better and 1.0 % or better for all mole ratios when the instrument is installed in a temperature-controlled environment and a variable-temperature environment, respectively. In the lab, the accuracy is 0.9 % or better for

[*]To whom correspondence should be addressed
[†]MIT/WHOI Joint Program
[‡]Woods Hole Oceanographic Institution
[¶]Wellesley College

Cite as:
Manning, CC, RHR Stanley, DE Lott (2016) Continuous measurements of dissolved Ne, Ar, Kr, and Xe ratios with a field-deployable gas equilibration mass spectrometer. *Anal. Chem.*, 2016, 88 (6), 3040–3048.
DOI: 10.1021/acs.analchem.5b03102

all gas ratios using air as the only calibration standard. In the field (and/or at greater levels of disequilbrium), the accuracy is 0.7 % or better for Ne/Kr, Ne/Ar, and Ar/Kr, and 2.5 % or better for Ne/Xe, Ar/Xe, and Kr/Xe using air as the only calibration standard. The field accuracy improves to 0.6 % or better for Ne/Xe, Ar/Xe, and Kr/Xe when the data is calibrated using discrete water samples run on a laboratory-based mass spectrometer. The e-folding response time is 90–410 s. This instrument enables the collection of a large number of continuous, high-precision and accuracy noble gas measurements at substantially reduced cost and labor compared to laboratory-based methods.

# Introduction

Noble gases are biologically and chemically inert, making them useful tracers of physical processes in the environment.[1] In water, measurements of dissolved noble gases in tandem with bioactive gases such as $O_2$ can be used to separate the effects of biological versus physical processes on the equilibrium state of gases, enabling accurate estimates of biological productivity.[2–4] Dissolved noble gas measurements can also be used to quantify oceanic processes such as gas ventilation in deep-water formation regions, diapycnal mixing, and sea ice melting and formation.[3,5–7] On land, measurements of noble gases in groundwater can be used to generate paleotemperature records and for studies of groundwater-aquifer and groundwater-ocean interactions.[8–10]

Traditional methods for measuring multiple noble gases in natural waters via mass spectrometry involve the collection of discrete samples and laboratory-based analysis. Sample processing and analysis is time-consuming (often multiple hours per sample) and requires specialized and expensive equipment. Currently, very few labs in the world are capable of high-precision and high-accuracy (1 % or better) measurements of Ne, Kr, and Xe in natural waters, and oceanic measurements of dissolved noble gases are sparse, particularly for Xe.[3,5,7,11,12]

Recently, the development of mass spectrometric methods for measurement of dissolved gases in the field[13–16] has led to high-resolution datasets of gases including $O_2$, Ar, $N_2O$ and dimethyl sulfide.[2,17,18] These instruments can analyze water in the field, in some cases eliminating the need

to transport discrete samples back to the laboratory for subsequent analysis. In this paper we describe the gas equilibration mass spectrometer (GEMS), a new method for on-site measurement of Ne, Ar, Kr, and Xe gas mole ratios in natural waters. We evaluate the precision and accuracy of the GEMS through comparison with a published laboratory-based method.[19] Our relatively low cost (~50 000 USD for the entire system in 2013) and low labor method will allow much higher throughput of noble gas measurement and will increase the number of scientists who are able to measure a suite of noble gases and use them as tracers for quantifying physical processes in the environment.

# Experimental section

The GEMS can be separated into the equilibration components ('wet side'), and the measurement components ('dry side') (Figure 1). In brief, the equilibration components include the following features: filtered water is pumped through a membrane contactor cartridge containing a gas-permeable membrane, the headspace of the cartridge is continuously recirculated and dried, and gas is sampled via a capillary at a very low flow rate and transferred to the mass spectrometer. A switching valve is used to alternate between sampling from the cartridge and sampling ambient air, for calibration. The measurement components include metal alloy getters for purifying the gas stream, a quadrupole mass spectrometer, vacuum pumps, and a laptop computer. We describe below the final configuration that gave us the best results. We encourage scientists who are interested in building their own systems to consult the Supporting Information, where we describe some alternative configurations that were less effective. The Supporting Information also includes tables of instrument settings (Tables S1–S2) suppliers and part numbers (Tables S3–S4) and photos and schematics of the instrument (Figures S5–S8).

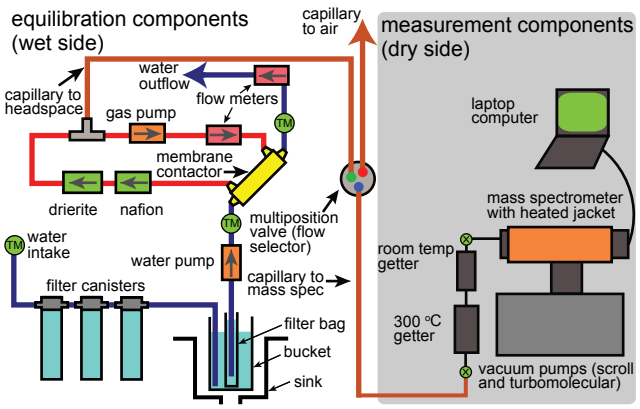


Figure 1: Schematic of the instrumental setup (not drawn to scale). See main text for description. See Figures S2–S4 for photos of the system.

## Equilibration components

For shipboard installation, water from the ship's underway seawater line passes through three 10" filter canisters containing reusable pleated filters (100, 20, and 5 $\mu$m nominal pore size) at a flow rate of ~30 cm$^3$ s$^{-1}$ and then into a bucket placed in a sink (Figure 1). Alternatively, any natural water source, such as water from a groundwater well or lake, can be continuously pumped with a submersible well pump, filtered, and used to fill the bucket. A two-layer filter bag consisting of 100 $\mu$m (outer) and 5 $\mu$m (inner) nominal pore size felt is placed inside the bucket. The filters are necessary to prevent the membrane contactor from clogging. Flexible PVC tubing and a gear pump is used to transfer water at a flow rate of ~18 cm$^3$ s$^{-1}$ from the filter bag to the membrane contactor and then to waste, down the sink drain (Figure 1). Our filter setup, water flow path, and gear pump is very similar to the configuration for the equilibrator inlet mass spectrometer developed by Cassar et al.(2009),[14] except that we use the larger filter canisters to prolong the life of the disposable felt filter bags, due to our higher water flow rates. The filter canisters are not necessary when performing lab experiments with distilled or tap water.

The membrane contactor cartridge (Liqui-Cel Extra-Flow 2.5 x 8, model G540) contains hollow, tubular membranes composed of porous, hydrophobic polyethylene fiber. The tubes, called lumens, are 300 $\mu$m diameter and the total membrane surface area is 1.4 m$^2$. Water flows through the membrane contactor, outside the lumens, and gas dissolved in the water transfers across the lumens

into the headspace (gas side) of the cartridge. Although liquid water does not cross the membrane, water vapor transfers through the pores and can condense on the headspace side of the membrane, reducing the gas transfer efficiency by clogging the pores.[20,21] Therefore, the headspace is continuously recirculated and dried to improve gas transfer efficiency across the membrane. The headspace flows at 1.8 $cm^3$ $s^{-1}$ through a Nafion tube surrounded by molecular sieves and cobalt chloride indicator (PermaPure DM-110-24), then through a small piece of flexible PVC tubing containing ~10 g of indicating Drierite ($CaSO_4$, 10-20 mesh), then through a T-shaped fitting with a capillary adapter for sampling the gas, and finally through a diaphragm pump before re-entering the headspace (Figure 1). These drying techniques were selected because they do not require any additional gas or power sources. The headspace is recirculated in the opposite direction to the water, i.e., water enters and gas exits at the bottom of the cartridge. The recirculation loop increases the effective headspace volume by less than 10 %, and therefore it likely has a negligible effect on the response time. Without drying, the headspace partial pressure of water vapor ($p_{H2O}$) is near saturation equilibrium, since water is observed to condense on the headspace side. With drying, $p_{H2O}$ in the headspace is somewhat lower and likely closer to ambient atmospheric $p_{H2O}$. We do not measure the gas humidity because, as discussed below, the vast majority of the water vapor is removed by the getters before entering the mass spectrometer.

A critical design principle of the gas equilibration mass spectrometer (GEMS) is that the gas in the headspace of the membrane contactor must be in equilibrium with the water flowing through the membrane contactor. If this condition is met, the gas mole ratios in water can be calculated from the measured headspace ratios, relative to air, and the gas solubility functions (Henry's law coefficients). At equilibrium, the headspace is composed of all the gases that are dissolved in the water, each at a partial pressure ($p$) yielding equilibrium with the water flowing through the membrane contactor. This partial pressure of each gas can be calculated from its Henry's law coefficient, which is a function of the temperature and salinity of the water. If air-equilibrated water flows through the cartridge, the pressure of each gas in the headspace is equal to its pressure in air. If water that is 5 % supersaturated in Ne flows through the cartridge, the partial pressure

of Ne will be 5 % higher in the headspace compared to air. When first setting up the membrane contactor, we recommend allowing water to flow through the cartridge for at least 1 h, to allow the headspace composition (which is initially air) to come into equilibrium with the water flowing through the cartridge.

To verify that the headspace is at a similar pressure to the ambient air, we temporarily placed a pressure measurement gauge (convectron), calibrated to air, in the headspace recirculation loop. We found that the headspace pressure was within ~1 % of ambient air pressure when sampling air-equilibrated water.

To maintain equilibrium, we ensure that the rate of gas flow out of the headspace and into the mass spectrometer is negligible relative to the rate of gas transfer across the membrane. We use a long, small-diameter capillary (0.05 mm ID, 5 m total length, deactivated fused silica) to achieve this low flow rate. The estimated gas flow rate through the capillary is $\sim 8 \times 10^{-5}$ cm$^3$ s$^{-1}$ (~7 cm$^3$ d$^{-1}$) based on a modified Hagen-Poiseuille equation. Cassar et al. (2009)[14] found that the Hagen-Poiseuille equation was a good approximation for capillary flow in a similar system. Calibration of the instrument is performed by periodically sampling air through a second capillary of the same dimensions.[14]

Accurate measurement of temperatures throughout the water flow path is critical, in order to correct for the effects of changes in temperature on the saturation state of each gas. The temperature is measured at the water intake (using a sensor with accuracy of ±0.05 °C), and immediately before and after the membrane contactor using two thermistors (accuracy ±0.1 °C). The average of these two temperatures is used as the equilibration temperature. The thermistors (temperature sensors) are shown as green circles labeled TM in Figure 1. We reduce the magnitude of the temperature change by placing foam insulation around the filter canisters, tubing, and the membrane contactor.

## Measurement components

A multiposition Valco valve is used to alternate between the two capillaries. The valve is connected to a 1 m long capillary to sample air, a 1 m long capillary to sample the headspace, and a common

4 m long capillary connected to the mass spectrometer. The valve to the mass spectrometer (Figure 1, blue circle) is always open, and the second open valve position switches from the headspace (red circle) to air (green circle) to perform a calibration. Sample gas flows from the membrane contactor (air), through the capillary and multiposition valve, through two chambers filled with reactive metal alloy getters and then into the ion source of the quadrupole mass spectrometer (Hiden HAL 3F RC201). Vacuum is provided by a combined turbomolecular and dry scroll pumping system (Agilent TPS-Compact). The pressure measured in the mass spectrometer is $\sim 1 \times 10^{-5}$ Pa while sampling air or the headspace of the membrane contactor.

Removal of unwanted gases such as $N_2$, $O_2$, and $H_2O$ from the gas stream greatly improves the detection limit by reducing molecule-molecule collisions within the mass spectrometer, and reduces matrix effects caused by differences in composition and pressure between the two gas streams. Published methods of noble gas analysis purify the gas stream using low temperature (cryogenic) traps and/or chemical purification.[19,22–24] In-line purification with getters is ideal for a portable system because it does not require any additional maintenance in the field, nor the transport of cryogenic liquids. We used two custom-fabricated getter chambers (cylindrical stainless steel containers) filled with SAES Getters St2002 pellets (Figures S7–S8). During operation, the first can is heated to 300 °C and contains 100 g of getter; the second can is kept at room temperature and contains 30 g of getter. The heated getter breaks the C-H bonds in $CH_4$, and adsorbs all other gases except for $H_2$ and the noble gases. The room temperature getter adsorbs $H_2$, from pure $H_2$ gas and from the decomposed $CH_4$, and also adsorbs all the other gases, at a lower efficiency compared to the heated getter. We selected alloy St2002 due to its superior $N_2$ removal efficiency (Figure S1). Reactivation of the getter surface is performed by heating both chambers to 400 °C for 1 hr, and is required roughly once per month (when the signal intensity for $N_2$ becomes greater than the signal intensity for $^{40}Ar$). The getter lasts approximately one year before replacement is needed. The temperature of both getter chambers is continuously recorded using thermocouples in contact with the heater elements. Using this purification method, >98 % of the non-noble gas content is removed from the gas stream before it enters the ion source, regardless of the initial gas

content (total pressure, humidity, and abundance of other gases).

The noble gases are measured with a quadrupole mass spectrometer operated with a secondary electron multiplier (SEM) detector. The mole ratios are determined by selected ion monitoring. Calibration with air, which has known and constant noble gas mole ratios,[25] is used to convert the averaged ion ratios to the deviation from saturation equilibrium. We measure Ne, Ar, Kr, and Xe. Helium is not measured because we found that He permeates through the capillary and/or the cartridge (see Supporting Information), and Rn is not measured because its concentration is too low (~6 orders of magnitude less abundant than Xe in seawater).

The Hiden Analytical instrument was selected because it has the ability to measure individual selected ions at different electron energies, in a repeated sequence, without a loss in stability. We measure $^{22}$Ne with a reduced electron energy to prevent formation of doubly charged $CO_2$, which is a potential isobaric interference. Although the getters remove >90 % of the $CO_2$, the signal intensity for $CO_2$ after purification is sufficient to interfere with the $^{22}$Ne measurement. Therefore, we prevent the formation of the doubly-charged ion $CO_2^{2+}$ by reducing the electron energy (cathode voltage) below 37 V, as done by Hamme and Emerson[26] (see Supporting Information). We measure $^{22}$Ne at an electron energy of 35 V and all other masses at an electron energy of 55 V (Table S1–S2). The precision and sensitivity for Ar, Kr, and Xe is improved at the higher electron energy.

For Ar, we analyzed $^{36}$Ar (0.337 % abundance) and/or $^{38}$Ar (0.0629 % abundance). The primary isotope, $^{40}$Ar, is 500–10 000 times more abundant in air than the other noble gases. The signal intensity for $^{40}$Ar is too high to be read accurately using the SEM at our operating pressure.[24] The signal intensities for $^{36}$Ar and $^{38}$Ar are at least 40 and 8 times higher, respectively, than the other noble gases we measure. In general, we found that measuring $^{38}$Ar was preferred because it could be measured on the same amplifier as $^{84}$Kr, whereas $^{36}$Ar had to be measured on a lower amplifier due to its higher abundance. By minimizing the range of signal intensities, we minimize nonlinearities in the detector response. For Kr, the primary isotope, $^{84}$Kr (57.0 % abundance) was chosen. For Xe, the least abundant gas, we measure both $^{129}$Xe and $^{132}$Xe (26.4 and 26.9 % abundance,

respectively), and take the average of the two signal intensities. Since Xe is the least abundant of the gases we measure, measuring both isotopes and taking the average reduces the noise compared to just measuring one isotope of Xe. Each measurement cycle (one measurement of each selected ion) takes ~1 min; see Tables S1–S2 for further details on the mass spectrometer settings.

We place a custom-fabricated heater jacket set to 50 °C around the manifold, to reduce the effects of room temperature change on the instrumental response, which is of particular concern when operating the instrument in the field, where there may be large fluctuations in ambient temperature. We use thermocouples to continuously monitor and record the room temperature and the manifold temperature. The mass spectrometer and vacuum pumps are connected to an uninterruptible power supply (UPS, Eaton 9130) to isolate them from power fluctuations.

The mass spectrometer data is acquired and saved using the manufacturer's software (MASsoft Pro 7). A custom Visual Basic program automates the valve switching between air and the headspace, and records temperatures and flow rates. The data from both programs is plotted in real time using Matlab.

The system described above was optimized for measurement of noble gas mole ratios. However, the equilibration components could potentially be used to equilibrate many other gases, given that we achieve full equilibrium of Ne, Ar, Kr, and Xe, which span a factor of 10 range in solubility. We have successfully obtained high-accuracy, high-precision measurements of $O_2$/Ar mole ratios using the system described above, with the getter chambers eliminated.

## Data analysis

In this section, we describe how to use the raw mass spectrometer data (extracted ion profile) to calculate the mole ratios of the gases dissolved in water. As discussed above, if the rate of gas removal from the headspace by the capillary is negligible relative to the rate of gas transfer across the membrane, then full equilibration of the gases between the water flowing through the membrane contactor and the headspace can occur.[13,14]

We use the GEMS to determine the mole ratio of two gases (and the deviation of this ratio from

equilibrium), rather than their individual concentrations.[14] If we recirculate air-equilibrated water through the membrane contactor, the measured ratios of any two noble gases are equivalent for the headspace versus air. However, the raw signal intensities for each gas in air versus the headspace are different by up to a few percent, and the magnitude of the offset can change with time. These offsets may be caused by slight differences in the rate of gas delivery to the mass spectrometer (e.g., due to differences in pressure between the headspace and air, or slight differences in the dimensions of the two capillaries), and/or differences in composition between the two gas streams causing matrix effects.[14,19] Although obtaining the individual concentrations would be ideal, the noble gas mole ratios can be effectively used to quantify physical processes.[3,11,27]

We use Henry's Law to determine the equilibrium molality of any inert gas, such as Ne

$$n_{Ne_{eq}} = p_{Ne_{air}} \cdot H_{Ne}(T, salinity) \tag{1}$$

where $n_{Ne_{eq}}$ is the molar concentration dissolved in water at equilibrium (mol kg$^{-1}$) and $p_{Ne_{air}}$ is the partial pressure of Ne in dry air (atm). $H_{Ne}$ is the Henry's Law solubility coefficient of Ne (mol kg$^{-1}$ atm$^{-1}$) and is a function of the water temperature and salinity.[28,29] We express the noble gas molar ratios in terms of the in situ deviation from the solubility equilibrium, often termed the saturation anomaly

$$\Delta\left(\frac{Ne}{Xe}\right) = \left[\frac{\left(\frac{n_{Ne}}{n_{Xe}}\right)_w}{\left(\frac{n_{Ne}}{n_{Xe}}\right)_{eq}} - 1\right] \times 100\%, \tag{2}$$

where $(n_{Ne}/n_{Xe})_w$ is the molar ratio of the gases dissolved in water and $(n_{Ne}/n_{Xe})_{eq}$ is the molar ratio of the gases in the water at saturation equilibrium. Here, we show how the saturation anomaly, $\Delta(Ne/Xe)$, can be determined from measurements of $(Ne/Xe)_{hs}$ and $(Ne/Xe)_{air}$, the ratios in the headspace and air, respectively. Following from Equation 1 the equilibrium gas ratio $(Ne/Xe)_{eq}$ is defined as

$$\left(\frac{Ne}{Xe}\right)_{eq} = \left(\frac{p_{Ne}}{p_{Xe}}\right)_{air} \left(\frac{H_{Ne}}{H_{Xe}}\right)_{T1} \tag{3}$$

where the subscript $T1$ indicates the in situ temperature (where the water was sampled). For

the membrane contactor, if the headspace is in equilibrium with the water passing through the cartridge, then we can calculate the ratio of the gases dissolved in water as

$$\left(\frac{Ne}{Xe}\right)_w = \left(\frac{p_{Ne}}{p_{Xe}}\right)_{hs} \left(\frac{H_{Ne}}{H_{Xe}}\right)_{T2}, \tag{4}$$

where the subscript $hs$ indicates the headspace and $T2$ indicates the equilibration temperature inside the membrane contactor. By substituting Eqns. 3 and 4 into Equation 2, we find

$$\Delta\left(\frac{Ne}{Xe}\right) = \left[\frac{\left(\frac{Ne}{Xe}\right)_{hs}\left(\frac{H_{Ne}}{H_{Xe}}\right)_{T2}}{\left(\frac{Ne}{Xe}\right)_{air}\left(\frac{H_{Ne}}{H_{Xe}}\right)_{T1}} - 1\right] \times 100\%. \tag{5}$$

Finally, using the definition of $(H_{Ne}/H_{Xe})$ which follows from from Equation 1 at $T1$ and $T2$, we obtain

$$\Delta\left(\frac{Ne}{Xe}\right) = \left[\frac{\left(\frac{Ne}{Xe}\right)_{hs}\left(\frac{Ne}{Xe}\right)_{eq,T2}}{\left(\frac{Ne}{Xe}\right)_{air}\left(\frac{Ne}{Xe}\right)_{eq,T1}} - 1\right] \times 100\%. \tag{6}$$

Thus, the deviation of the gas ratios from solubility equilibrium can be determined by alternating between measurements of the noble gases in air and the headspace. The ratio in air is measured periodically (e.g., for a 40 min block after every 100–300 min of water sampling). We take the average of all the air measurements in each block (omitting the first and last 5 min), and then apply a linear interpolation between each pair of air measurements to calculate the air ratio at the time of each headspace measurement, as done by Cassar et al. (2009)[14] for $O_2$/Ar.

We measure $T1$ in situ, wherever the water is sampled. For example, on a ship $T1$ is measured using a sensor mounted on the hull of the ship adjacent to the seawater intake. $T2$ is determined from the average of two thermistors in the water flow path: one immediately before and one immediately after the membrane contactor. The salinity is measured once and we assume the in situ and equilibration salinities to be the same. We have observed $T2$ to be up to 1.0 °C greater than $T1$, which results in a ~2.5 % correction to the calculated $\Delta(Ne/Xe)$ value.

# Results and Discussion

## Precision

To determine the precision of the GEMS, we recirculated water from a temperature-controlled bath through the membrane contactor and collected data while continuously sampling from the headspace only. We then performed calculations to simulate the process of switching between air and the headspace (Figure 2). For these calculations, we used the ratios calculated from the raw signal intensity (extracted ion profile), without adjustment to the molar abundances in water or air. For example, the precision of the Ne/Kr ratio was calculated from the signal intensity of $^{22}$Ne/$^{84}$Kr. We applied a linear interpolation to the raw ratio data, based on averaging 30 min of data every 340 min (i.e., simulating a 40 min measurement in air, with the first and last 5 minutes removed before averaging). This timing is identical to the timing of the lab-based accuracy experiment described below. A 7-min running mean filter was then applied to the 300-min intervals of data; this averaging time is equal to the e-folding response time of Ne, which has the slowest response rate of the gases we measure. We define the precision as the relative standard deviation (RSD) of the difference between the filtered ratios and the interpolated ratios. In a temperature-controlled room, the precision is 0.7 % or better for all gas ratios (0.7, 0.5, 0.5, 0.6, 0.2, and 0.6 % for Ne/Xe, Ne/Kr, Ne/Ar, Ar/Xe, Ar/Kr and Kr/Xe, respectively). We report the precision for all ratios as lighter gas/heavier gas for consistency. The relative precision (% RSD) is the same for Ne/Xe as for Xe/Ne. Because the different noble gases we measure have different abundances and physical properties, the gas ratios have varying precision and accuracy. We report the precision and accuracy for all gas combinations since the utility of each gas ratio to study environmental processes depends on the specific gases and on the precision/accuracy for that specific ratio. We got very similar results (precision of 0.7 % or better for all gas ratios) when we measured air in the lab continuously, instead of water. When determining the precision from measurements of the headspace or air, we determine how similar each measurement is to the expected value. We did not alternate between measuring air and the headspace because if air was being used to calculate the

expected headspace ratios, then any disequilibrium in the water with respect to air would bias the calculated precision.

In the field, the precision was somewhat worse, likely due to room temperature change. When we installed the mass spectrometer in an unheated garage, the mass spectrometer signal intensity for each ion drifted with temperature, despite the heater jacket on the manifold. In a variable-temperature environment, air calibrations should be performed more frequently. To determine the precision, we measured air continuously and then averaged 30 min of data every 150 min. In this environment, the precision while measuring air was1.0 % or better for all gas ratios (1.0, 0.6, 0.5, 0.9, and 0.8 % for Ne/Xe, Ne/Kr, Ne/Ar, Ar/Xe, Ar/Kr and Kr/Xe, respectively). We did not determine the precision while measuring water in the field because we did not have access to a temperature-controlled water bath.

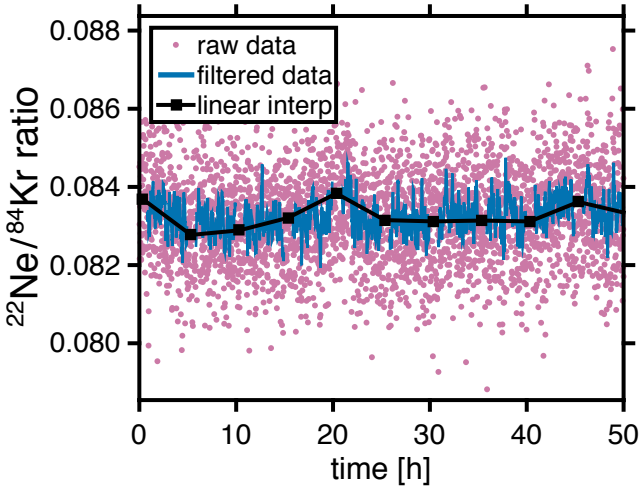


Figure 2: Measurements of $^{22}$Ne/$^{84}$Kr signal intensity while sampling the headspace and recirculating air-equilibrated water through the membrane contactor. The pink dots show individual data points, the black line is a linear interpolation based on averaging 30 min of data every 340 min, and the blue line is the data after applying a 7-min running mean filter. The precision is calculated from the difference in magnitude between the blue and black lines.

## Accuracy

To determine the accuracy of the GEMS, we compared the GEMS data to a published method[19] (discrete samples analyzed by a laboratory-based mass spectrometer) during experiments in the

field and the lab. In the lab, using the GEMS, we recirculated water from an insulated 0.12 $m^3$ tank filled with distilled water that was open to the lab air. The water in the tank was constantly mixed using a submersible pump at the bottom of the tank. The temperature of the water was changed during the experiment. A filter sock was placed directly into the water bath and a gear pump connected to tubing was used to withdraw water from the filter sock and pump it through the membrane contactor. For the discrete samples, water was withdrawn using a spigot on the bath. Inside the tank, the spigot was connected to tubing, with the open end of the tubing placed next to the filter sock, so that the water removed for discrete sample collection would be near the water that entered the membrane contactor. Outside the tank, the other end of the spigot was connected to tubing for sampling. In the lab experiment, we collected and analyzed one discrete sample at 10 time points over five days.

In the field experiment, water was pumped from Waquoit Bay, MA, using a submersible well pump. The water passed through the canister filters and then into a bucket to overflow, as shown in Figure 1. After the canister filters and before the bucket, a sampling valve was installed and used to collect the discrete samples. For this experiment, we collected and analyzed one discrete sample at eight time points over eight days.

The discrete samples were collected in copper tubes, sealed with a cold pressure welder and extracted in the lab.[30] Noble gas abundances were measured on a pulse counting quadrupole mass spectrometer.[19] This method determines the concentration of each gas (in $cm^3_{STP}\ g^{-1}$ or $mol\ kg^{-1}$), with a combined standard uncertainty of 0.2–0.3 % for each gas. In order to compare the GEMS data to the discrete samples, we must convert the GEMS measurements of saturation anomalies to mole ratios. Therefore, the choice of solubility function directly influences our estimates of the accuracy of the GEMS.

For Ne and Ar, we used the solubility determinations of Hamme and Emerson (2004)[28] who determined the solubilities of Ne and Ar in fresh water and seawater with an accuracy of 0.30 and 0.13 % respectively, by equilibration with air. For Kr and Xe in fresh water (the lab experiment), we used the solubility determinations of Benson and Krause (1976)[29] who determined solubilities

of all five stable noble gases in freshwater (but not salt water) with a stated accuracy of 0.1–0.2 %. For the field experiment (sampling seawater), we used the solubility of Weiss and Kyser (1978) for Kr,[31] and the solubility of Wood and Caputi (1966)[32] for Xe, fit by Hamme following the procedure in Hamme and Emerson (2004), who determined the solubilities in both fresh water and seawater.[28] Recent works have drawn the seawater solubilities of Kr and Xe into question because they are not consistent with oceanic data and have not been verified by multiple investigators.[7] Thus the Kr and Xe solubilities of Weiss and Kyser and Wood and Caputi have uncertainties of 1–2 %,[7,12] which results in increased uncertainty in our accuracy estimates during the field experiment for all mole ratios except Ne/Ar.

We define the accuracy as the average magnitude (absolute value) of the relative percent difference between the GEMS and discrete samples, with both datasets expressed in terms of gas mole ratios. We filtered the GEMS data with a 7-min running mean filter and then calculated the average mole ratios over a 7-min period centered around the time each discrete sample was collected. The choice of averaging time (from 3–15 min) did not significantly affect the estimated accuracy. The mole ratios obtained by the GEMS are determined from the measured saturation anomaly and the gas solubility at the in situ salinity and temperature.

In the lab experiment, the relative accuracy of the GEMS was 0.9 % or better for all gas mole ratios (Figure 3). The experimentally-determined accuracy was 0.8, 0.4, 0.9, 0.8, 0.8, and 0.6 % for the mole ratios of Ne/Xe, Ne/Kr, Ne/Ar, Ar/Xe, Ar/Kr, and Kr/Xe respectively. The relative percent accuracy is the same for Ne/Xe as for Xe/Ne, and likewise for the other gas mole ratios.

In the field experiment, the accuracy of the GEMS was 0.6, 0.7, and 0.4 % for Ne/Kr, Ne/Ar, and Ar/Kr (Figure S3). The accuracy of the ratios with Xe was substantially worse: 2.5, 2.0, and 2.4 % for Ne/Xe, Ar/Xe, and Kr/Xe, respectively. However, we found that we could improve the accuracy for the ratios with Xe by using the discrete samples to calibrate the GEMS (Figures S2–S4). We plotted the measured ratio, normalized to equilibrium for the GEMS versus the discrete samples and calculated a linear fit. The slope, $m$, and intercept, $b$ were used to calibrate the GEMS data.

$$\left[\frac{\left(\frac{n_{Ne}}{n_{Xe}}\right)_w}{\left(\frac{n_{Ne}}{n_{Xe}}\right)_{eq}}\right]_{discrete} = m\left[\frac{\left(\frac{n_{Ne}}{n_{Xe}}\right)_w}{\left(\frac{n_{Ne}}{n_{Xe}}\right)_{eq}}\right]_{GEMS} + b \quad (7)$$

The $R^2$ values for the fit were 0.93, 0.85, and 0.73 for Ne/Xe, Ar/Xe, and Kr/Xe, respectively (Figure S2). Using this technique to adjust the GEMS data, the accuracy became 0.6, 0.4, and 0.4 % for Ne/Xe, Ar/Xe, and Kr/Xe, respectively. Similarly, with calibration, the accuracy of the lab measurements also improved somewhat, to 0.6, 0.4 and 0.4 % for Ne/Xe, Ar/Xe, and Kr/Xe, respectively. Some of the error observed in the field may be associated with errors in the solubility of Kr and Xe. However, since the offset between the GEMS and discrete samples is not constant and seems to vary as a function of the magnitude of disequilibrium, not all of it can be explained by solubility errors.

We conclude that the GEMS can reliably obtain accuracy of 0.9 % or better for Ne/Kr, Ne/Ar, and Ar/Kr using air as the only calibration standard. For Xe, if accuracy of 0.9 % or better is desired, obtaining some discrete samples for calibration purposes is recommended.

We believe the reduced accuracy for Xe in the field experiment may be related to matrix effects.[19] Variability in the total pressure and/or the pressure of specific molecules may cause nonlinearities in the relationship between gas pressure and signal intensity at the detector (e.g., due to altering the ionization efficiency for the gas of interest). Xe is likely to be the most sensitive to these matrix effects because it is the least abundant gas we measure (closest to the detection limit), and since its saturation state is the most variable.[7,12] In unpurified air, the mole fractions of $O_2$ and $N_2$ are $\sim 10^9$ times greater than Xe . Therefore, even though the getters remove >98 % of the active (non-noble) gas content, the pressure of $N_2$ and $O_2$ is still far greater than the pressure of Xe after purification. Furthermore, in the field, biogenic gases such as $O_2$ and $CO_2$ will likely be more variable in abundance, and farther from equilibrium, compared to the lab experiment performed with distilled water. Therefore, we expect greater differences between the headspace and air composition in the field, leading to larger matrix effects.

Additionally, even if we could remove 100 % of the active gas, the pressure of $^{40}Ar$ would still

be 300 000 times greater than the pressure of $^{129}$Xe, and therefore the measured pressure of Xe may be affected by changes in the pressure of Ar.[19] A matrix effect caused by other noble gases may be more apparent at larger deviations from equilibrium. In our field dataset, the noble gas mole ratios were on average farther from equilibrium, and also had larger maximum magnitudes compared to the lab dataset. For example, the largest saturation anomalies measured for Ne/Xe, Ar/Xe, and Kr/Xe were 6.4, 3.9, and 3.1 % in the field and 4.3, 1.7, and 2.1 % in the lab, respectively, based on the discrete samples.

Notably, precision and accuracy are also degraded when the instrument experiences vibrations, such as on a ship (see Supporting Information).

Since we only analyzed one sample at each time point, we cannot determine whether any of the discrete samples may be inaccurate due to sampling or measurement problems; however, by using samples at 8–10 time points, we believe we have a good estimate of the overall accuracy. Comparing the two methods has an additional source of error: the discrete samples capture the instantaneous gas composition at the time the tube was sealed, whereas the GEMS averages over several minutes, with the e-folding time varying for each gas. The GEMS achieves similar accuracy to other methods that are much more expensive and labor-intensive.

## Equilibration timescale

When sampling the headspace, the signal intensity for each selected ion reflects a weighted average of the concentration over the equilibration timescale of the system. To determine the equilibration timescale, we switched between sampling water of two different gas compositions: air-equilibrated water and freshly distilled water. We fit the instrument response to a kinetic equation.[14] The signal intensity or concentration, C, for each noble gas can be modeled as

$$C_t = [C_i - C_f]exp(-t/\tau) \tag{8}$$

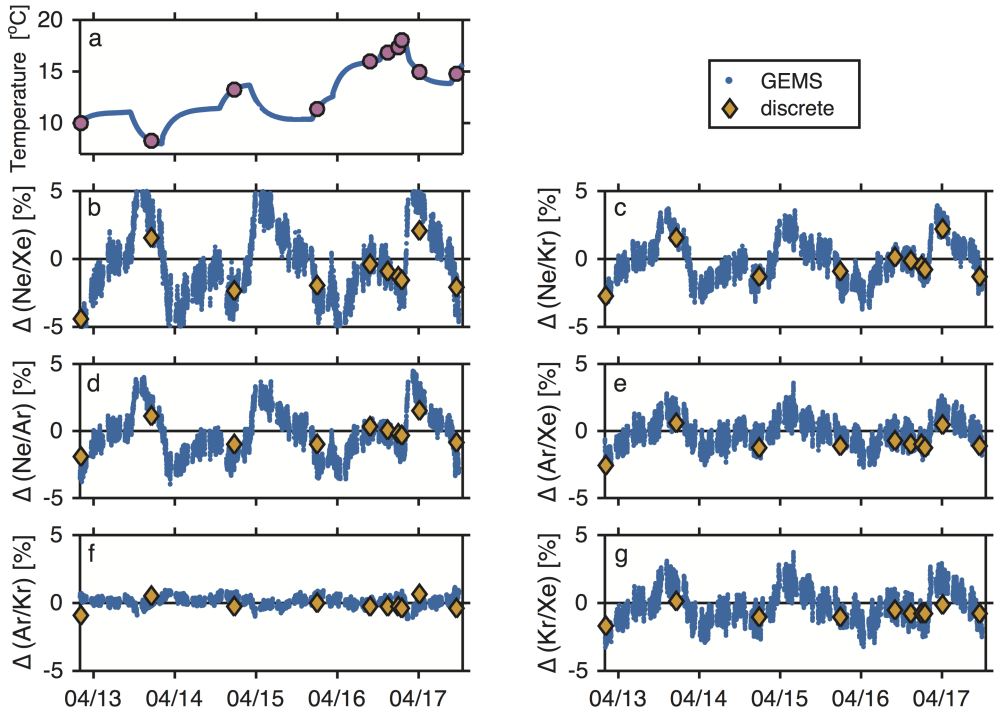


Figure 3: Results of a lab experiment to determine the accuracy of the GEMS. a) In situ temperature throughout the experiment (blue line) and the time each sample was collected (pink circles). b-g) Individual measurements by the GEMS filtered with a 7-min running mean filter (blue dots). Discrete samples (yellow diamonds), with the measured concentration converted to saturation anomalies. The height of the diamonds is equal to the measurement uncertainty.

where $C_i$ is the initial signal intensity (before switching the water composition), $C_f$ is the final intensity (after stabilization), $C_t$ is the intensity at any time $t$, and $\tau$ is the e-folding time of the instrument. Specifically, $\tau = t_{1/2} / \ln(2)$, with $t_{1/2}$ the time at which the signal intensity is halfway between $C_f$ and $C_t$. By rearranging equation 8, we can plot the data as a linear equation of the form $y = mx$ where $x = t$, $m = \tau^{-1}$, and

$$y = \ln\left(\frac{C_t - C_f}{C_i - C_f}\right). \tag{9}$$

For water at 20 °C and a water flow rate of 18 $cm^3$ $s^{-1}$, the e-folding times were found to be 410(54) s for Ne, 240(80) s for Ar, 190(80) s for Kr, and 90(10) s for Xe, where the numbers in parentheses are the standard uncertainty (Figure 4). These estimates are based on at least three measurements of the e-folding time for each gas; each measurement took ~2 h. The e-folding time increases with decreasing solubility. A greater proportion of the lower solubility gas must transfer between the water and the headspace in order for the two phases to re-equilibrate, causing the equilibration time to increase. Other investigators have noticed that lower solubility gases equilibrate less efficiently across Liqui-Cel membrane contactors.[14]

## Pilot field study

To demonstrate the utility of the GEMS, we conducted a pilot field study in Waquoit Bay, MA, USA. We installed the mass spectrometer and laptop in an unheated boathouse, and we installed the equilibration components just outside the boathouse. The filter and bucket were placed on a bench, and the remainder of the equilibration equipment was installed inside a wooden box to shelter it from precipitation. A hole in the the wall of the boathouse was used to connect the capillary between the multiposition valve and the mass spectrometer.

To sample water, we deployed a submersible well pump ~60 m offshore, in an average water depth of 1 m. The water pump and two temperature/salinity/depth sensors (RBR Concerto) were attached to a hollow PVC pipe mounted on a cement block. The water pump was installed with

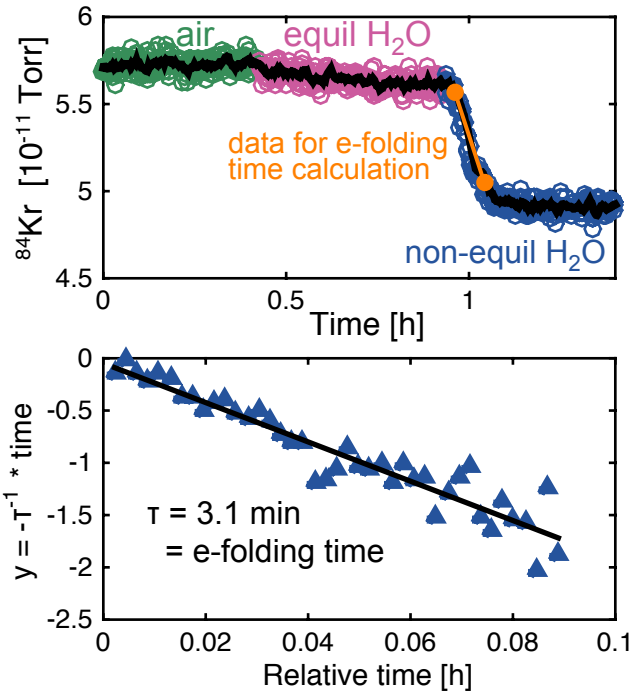


Figure 4: Results of an experiment to determine the equilibration timescale for each gas. a) $^{84}$Kr signal intensity during an experiment switching from air, to equilibrated water, to non-equilibrated water. The orange circles and line show the portion of the data that is used to calculate the e-folding time. b) Calculation of the e-folding time from a linear regression of $y = -\tau^{-1}t$, with $\tau$ the e-folding time and $t$ the time.

the intake at an average depth of 0.4 m, and the temperature/salinity/depth sensors were installed at an average depth of 0.4 and 0.8 m. An additional temperature sensor ~1 m above the water level was attached to the PVC pipe, to monitor air temperature. Wind speed data was taken from the Waquoit Bay Carriage House weather station, 200 m north (inshore) of the water pump.[33]

The GEMS collected data for one month. In Figure 5, we show the data from December 16–24, the time period when discrete samples were collected for method validation purposes. We typically checked on the system twice per day (morning and early evening), and it otherwise operated unattended. During these checks we replaced the filter socks (roughly once per day), replaced the canister filters (once per week), and replaced the dessicant and membrane contactor (once every five days). We also plotted the mass spectrometer data, flow rates, and temperatures, to verify that the system was operating as intended. We obtained a near-continuous time-series with occasional gaps resulting from the submersible pump coming out of the water at the lowest tides (e.g., midnight on Dec 19 and afternoon on Dec 21 in Figure 5). This type of study (sub-hourly measurement frequency, over a month) would not be practical with traditional sampling and analysis methods.[13]

In Figure 5, the GEMS data for $\Delta$(Ne/Xe) was calibrated using the discrete samples, and the other data is unadjusted. The error bars for $\Delta$(Ne/Xe) and $\Delta$(Ar/Kr) are larger in the field compared to the laboratory-based experiment, due to the larger uncertainties in the seawater solubility of Kr and Xe compared to the fresh water solubility. See the Accuracy section for more details.

The precision, accuracy, and response time of the system were sufficient to resolve substantial variability in noble gas saturation anomalies throughout the time-series. This variability was associated with changes in wind speed, water temperature, and air temperature (Figure 5). To determine whether the observations were consistent with our scientific understanding of physical controls on gas saturation state, we used a simple model. The model was forced with wind speed, temperature, and salinity observations, and the gas exchange parameterization of Nicholson et al. (2011),[27,34] which includes separate terms for diffusive and bubble-mediated gas exchange. We assumed a fixed 1 m water depth. We initialized the model on Dec 16, 12:30 pm using the measured saturation anomalies of the first discrete sample. This model is an oversimplification because

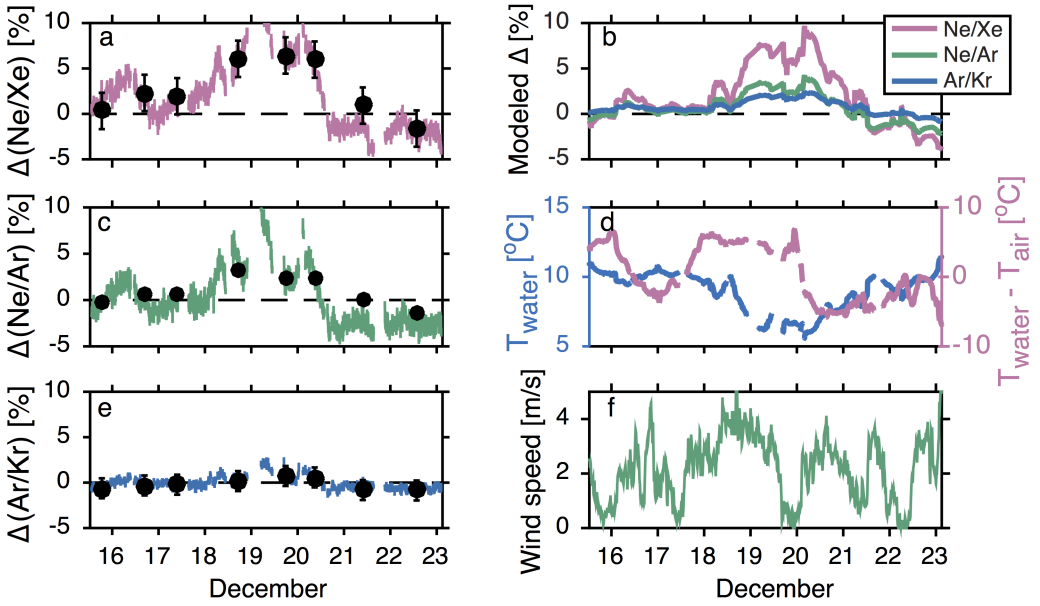


Figure 5: GEMS and discrete measurements of a) Δ(Ne/Xe), c) Δ(Ne/Ar), and e) Δ(Ar/Kr) in Waquoit Bay, MA. The Ne/Xe data has been calibrated using discrete samples, as described in the Accuracy section. b) Modeled gas distributions forced by the measured temperature, salinity, and wind speed. d) Variability in water temperature (blue line) changes the measured saturation anomaly, and the air-water temperature difference (pink line) affects the air-sea gas flux. e) Wind speed also affects the gas flux. Date ticks represent midnight local time.

it does not account for the movement of water masses (e.g., due to tides) and the variable water depth. However, the model helps us to determine how much of the variability can be explained by air-sea gas exchange and changes in temperature/salinity.

The model predicted many similar features to the observations. For example, the model and observations show similar amplitude in the saturation anomalies, with Ne/Xe having the widest range in saturation anomalies and Ar/Kr the least. Additionally, the timing of changes is similar in the model and data. For example, the model and data show the saturation anomalies increasing from near-equilibrium to positive values on December 18–20, and decreasing from positive values to negative values on December 20–21. The changes in saturation anomalies are linked to changes in the water temperature and the air-water temperature difference. High resolution data such as this could be used to examine other processes such as tidally driven flows/mixing (e.g., by combining the GEMS with current velocity measurements) and to infer the rates of biological processes (e.g., by combining the GEMS with $O_2$ measurements). In the Supporting Information, we de-

scribe in detail several potential applications of the GEMS, including lab-based tank experiments, introduced tracer studies, and parameterizing physical versus biological gas fluxes.

## Comparison with other published methods

The GEMS dramatically increases throughput, decreases labor, and decreases costs compared to traditional discrete sampling and analysis methods. The GEMS has improved accuracy and time resolution compared to another portable method that measures Ar and Kr, but not Ne or Xe.[13] The accuracy is similar to[22,35,36] or somewhat less accurate than[7,19] laboratory-based methods that cause much higher cost and labor. Additionally, the laboratory-based methods with higher precision require much more expensive instrumentation (over 250 000 USD), have higher analysis costs (~500 USD per sample), and have lower sample throughput (~4 samples per day), since each sample takes several hours to extract and analyze. In contrast, our system is less expensive to build (~50 000 USD in 2013), requires minimal consumables, and can collect an endless number of samples with a time resolution of 90–410 s. Thus, the GEMS enables continuous, real-time measurements of four noble gases, with a sampling frequency (sub-hourly) that would be challenging to achieve via traditional methods.[13]

The main disadvantage is that the described GEMS system does not determine the gas concentrations; instead it determines their mole ratios. In the future, we plan to test modifications to the GEMS that will enable the determination of the gas concentrations, in addition to their mole ratios. For example, the GEMS could be used along with a second mass spectrometer measuring $O_2$/Ar ratios (e.g., an equilibrator inlet mass spectrometer,[14] a membrane inlet mass spectrometer,[16,18,37] or the GEMS system described above, with the getter chambers eliminated) and a well-calibrated sensor for $O_2$ concentration. The $O_2$/Ar ratio and the $O_2$ concentration could be used to derive the Ar concentration,[6,38] and the other noble gas concentrations could be determined from the GEMS noble gas ratios and the Ar concentration. Another potential modification is changing the system to measure individual samples, instead of a continuous gas stream.[13,24]

# Conclusions

We have described the gas equilibration mass spectrometer (GEMS), a new field-deployable method for continuous measurement of the mole ratios of four noble gases (Ne, Ar, Kr, and Xe) dissolved in water. In the lab, the precision is 0.7 % or better, and in a variable-temperature environment the precision is 1.0 % or better. The accuracy is 0.9 % or better for all gas ratios in the lab. In the field (and/or at greater disequilibrium) the accuracy is 0.7 % or better for Ne/Kr, Ne/Ar, and Ar/Kr and 2.5 % or better for Ne/Xe, Ar/Xe, and Kr/Xe, but can be improved through calibration with discrete samples to 0.6 % or better.

## Acknowledgement

The authors thank Kevin Cahill, Josh Curtice, James Rassman, and Zoe Sandwith for their contributions to lab and field work, Bill Jenkins for processing the noble gas data from discrete samples, and David Nicholson for discussions about the field data. The manuscript was improved thanks to the thoughtful suggestions of two anonymous reviewers. Funding was provided by NSF award OCE-1060840 and a WHOI Innovative Technology award to RHRS, and scholarships from NSERC and CMOS to CCM.

## Supporting Information Available

Lists of suppliers and parts numbers, photos of the system, a diagram of the getter chambers, descriptions of some alternative configurations of the system, and further details on the calibration of field data.

This material is available free of charge via the Internet at `http://pubs.acs.org/`.

## References

(1) Stanley, R. H.; Jenkins, W. J. *The Noble Gases as Geochemical Tracers*; Springer, 2013; pp 55–79.

(2) Stanley, R.; Kirkpatrick, J.; Cassar, N.; Barnett, B.; Bender, M. *Global Biogeochem. Cycles* **2010**, *24*, GB4001.

(3) Nicholson, D.; Emerson, S.; Caillon, N.; Jouzel, J.; Hamme, R. C. *J. Geophys. Res. Oceans* **2010**, *115*.

(4) Stanley, R. H.; Jenkins, W. J.; Doney, S. C. *J. Mar. Res.* **2006**, *64*, 267–295.

(5) Loose, B.; Jenkins, W. J. *Geophys. Res. Lett.* **2014**, *41*, 2835–2841.

(6) Eveleth, R.; Timmermans, M.-L.; Cassar, N. *J. Geophys. Res. Oceans* **2014**, *119*, 7420–7432.

(7) Hamme, R. C.; Severinghaus, J. P. *Deep Sea Res. I* **2007**, *54*, 939–950.

(8) Aeschbach-Hertig, W.; Solomon, D. *The Noble Gases as Geochemical Tracers*; Springer, 2013; pp 81–122.

(9) Castro, M. C.; Goblet, P.; Ledoux, E.; Violette, S.; Marsily, G. *Water Resour. Res.* **1998**, *34*, 2467–2483.

(10) Stute, M.; Schlosser, P. *Climate Change in Continental Isotopic Records* **1993**, 89–100.

(11) Hamme, R.; Emerson, S. *Geophys. Res. Lett.* **2013**, *40*, 1149–1153.

(12) Stanley, R. H. R.; Jenkins, W. J.; Lott, D. E.; Doney, S. C. *J. Geophys. Res. Oceans* **2009**, *114*.

(13) Machler, L.; Brennwald, M. S.; Kipfer, R. *Environ. Sci. Technol.* **2012**, *46*, 8288–8296.

(14) Cassar, N.; Barnett, B.; Bender, M.; Kaiser, J.; Hamme, R.; Tilbrook, B. *Anal. Chem.* **2009**, *81*, 1855–1864.

(15) Kameyama, S.; Tanimoto, H.; Inomata, S.; Tsunogai, U.; Ooki, A.; Yokouchi, Y.; Takeda, S.; Obata, H.; Uematsu, M. *Anal. Chem.* **2009**, *81*, 9021–9026.

(16) Virkki, V. T.; Ketola, R. A.; Ojala, M.; Kotiaho, T.; Komppa, V.; Grove, A.; Facchetti, S. *Anal. Chem.* **1995**, *67*, 1421–1425.

(17) Marandino, C.; De Bruyn, W. J.; Miller, S. D.; Saltzman, E. S. *Atmos. Chem. Phys.* **2009**, *9*, 345–356.

(18) Tortell, P. *Limnol. Oceanogr.: Methods* **2005**, *3*, 24–37.

(19) Stanley, R. H. R.; Baschek, B.; Lott, D. E.; Jenkins, W. J. *Geochem. Geophys. Geosyst.* **2009**, *10*, Q05008.

(20) Lv, Y.; Yu, X.; Tu, S.-T.; Yan, J.; Dahlquist, E. *J. Membr. Sci.* **2010**, *362*, 444–452.

(21) Wang, R.; Zhang, H.; Feron, P.; Liang, D. *Sep. Purif. Technol.* **2005**, *46*, 33–40.

(22) Sano, Y.; Takahata, N. *J. Oceanogr.* **2005**, *61*, 465–473.

(23) Severinghaus, J. P.; Grachev, A.; Luz, B.; Caillon, N. *Geochim. Cosmochim. Acta* **2003**, *67*, 325–343.

(24) Visser, A.; Singleton, M. J.; Hillegonds, D. J.; Velsko, C. A.; Moran, J. E.; Esser, B. K. *Rapid Comm. Mass Spectrom.* **2013**, *27*, 2472–2482.

(25) US Standard Atmosphere. 1976.

(26) Hamme, R. C.; Emerson, S. R. *Mar. Chem.* **2004**, *91*, 53–64.

(27) Nicholson, D. P.; Emerson, S. R.; Khatiwala, S.; Hamme, R. C. An inverse approach to estimate bubble-mediated air-sea gas flux from inert gas measurements. Proceedings of the 6th International Symposium on Gas Transfer at Water Surfaces, Kyoto University Press, Kyoto, Japan. 2011.

(28) Hamme, R.; Emerson, S. *Deep-Sea Res. I* **2004**, *51*, 1517–1528.

(29) Benson, B. B.; Krause Jr, D. *The Journal of Chemical Physics* **1976**, *64*, 689–709.

(30) Jenkins, W.; Lott, D.; Cahill, K.; Curtice, J.; Landry, P. *Sampling and measuring helium isotopes and tritium in seawater*; 2010, IOCCP Report No. 14.

(31) Weiss, R. F.; Kyser, T. K. *J. Chem. Eng. Data* **1978**, *23*, 69–72.

(32) Wood, D.; Caputi, R. *Solubilities of Kr and Xe in fresh and sea water*; Technical report, U.S. Naval Radiological Defense Laboratory, San Francisco, CA, 1966.

(33) NOAA National Estuarine Research Reserve System System-wide Monitoring Program, Centralized Data Management Office Website. `http://www.nerrsdata.org`, Accessed January 1, 2016.

(34) Manning, C. C.; Nicholson, D. P. gas_toolbox: MATLAB code used in Manning et al. GTWS-7 proceedings. Zenodo. `http://dx.doi.org/10.5281/zenodo.45293`, 2016.

(35) Brennwald, M. S.; Hofer, M.; Kipfer, R. *Environ. Sci. Technol.* **2013**, *47*, 8599–8608.

(36) Beyerle, U.; Aeschbach-Hertig, W.; Imboden, D. M.; Baur, H.; Graf, T.; Kipfer, R. *Environ. Sci. Technol.* **2000**, *34*, 2042–2050.

(37) Kana, T. M.; Darkangelo, C.; Hunt, M. D.; Oldham, J. B.; Bennett, G. E.; Cornwell, J. C. *Anal. Chem.* **1994**, *66*, 4166–4170.

(38) Hamme, R. C.; Cassar, N.; Lance, V. P.; Vaillancourt, R. D.; Bender, M. L.; Strutton, P. G.; Moore, T. S.; DeGrandpre, M. D.; Sabine, C. L.; Ho, D. T.; Hargreaves, B. R. *J. Geophys. Res.* **2012**, *117*, C00F12.

# Graphical TOC Entry